Fluorescence of Water-Soluble Fullerenes in Biological Systems

Sijie Lin,[1] Donovan X. Jones,[2] Andrew S. Mount,[3] Pu Chun Ke[4]*

Laboratory of Single-Molecule Biophysics and Polymer Physics
[1]School of Materials Science and Engineering
[2]Department of Bioengineering
[3]Department of Biological Sciences
[4]Department of Physics and Astronomy, pcke11@clemson.edu
Clemson University, Clemson, SC 29634, USA

ABSTRACT

Fullerene C_{70} has been solubilized in aqueous solutions using phenol gallic acid. The supermolecule of C_{70}-gallic acid is hypothesized to be assembled via pi-stacking as well as by caging of gallic acid around single or multiple C_{70}. When excited with light, C_{70}-gallic acid exhibited two prominent fluorescence peaks at 540 nm and 719 nm. Using confocal fluorescence microscopy we have observed the translocation of C_{70}-gallic acid and their consequent green fluorescence in CHO cells, oyster tissue, and living organism Ceriodaphnia. The resistance of C_{70}-gallic acid to photobleaching combined with the antioxidation property of gallic acid can potentially be utilized for novel biological imaging, sensing, and drug delivery.

Keywords: fullerenes, gallic acid, solubility, fluorescence

1 INTRODUCTION

Cage-like fullerene molecules represent a class of carbon-based nanomaterials with unique structural, mechanical, and electronic properties. When interacting with biological systems, fullerenes have found use in such applications as neuroprotective agents [1], HIV-1 protease inhibitors [2], antioxidants [3], X-ray contrast enhancers [4], and drug delivery transporters [5]. Due to their mutual van der Waals interaction, fullerenes readily accumulate, and their aggregates can facilitate electron transfer across cell membranes [6,7], a phenomenon which can impact photosynthesis and biomedicine.

The absorption spectra of C_{60} and C_{70}, two of the most abundant forms of fullerenes, are rather similar in the ultraviolet region. In the visible range, C_{70} displays markedly stronger absorption than C_{60} due to its elongated form and reduced symmetry which relax the forbidden electronic transitions [8,9]. As a result, in crystal phase or dissolved in organic solvents such as toluene or benzene, C_{70}, and to a lesser extent C_{60}, can be photoexcited to induce multiple fluorescence bands from visible to near infrared [8-12]. However the fluorescence of fullerenes in organic solvents is noticeably weak, possibly resulting from rapid intersystem crossing and small fluorescence radiative rate constants [8,9].

Because of their inert surface structures, fullerenes are only weakly soluble in water. As a result, while the photophysical properties of fullerenes in aqueous solutions have not been extensively studied, they could have great potential for biosensing and imaging. Consequently this paper is to demonstrate the solubilization of fullerenes in aqueous solutions with gallic acid and perform cellular to organism-level imaging using the unique fluorescence properties of supramolecular complex C_{70}-gallic acid.

2 RESULTS AND DISCUSSION

2.1 Absorption of C_{70}-Gallic Acid

We have solubilized C_{70} in water using phenol antioxidant gallic acid (see Figure 1a inset) [13,14]. The absorption spectrum of gallic acid was measured using a spectrophotometer (Figure 1a). The UV absorbance of C_{70}-gallic acid vs. concentration was read at 384 nm where gallic acid had a minimal contribution. A plateau of absorbance was found at approximately 1 mg/mL, indicating the saturation of C_{70} solubility (Figure 1 b). This value is consistent with our observation of dark precipitates for samples of 1 mg/mL or higher.

The complex of C_{70}-gallic acid is hypothesized to be assembled via pi-stacking and its solubility afforded by the three hydroxyls and one carboxyl of each gallic acid molecule. In addition, gallic acid molecules may also cage around C_{70} molecule(s) via hydrogen bonds to elicit an improved solubility, analogous to the way colloidal clusters are formed by water surrounding fullerenes [15]. According to our transmission electron microscopy (TEM) study each C_{70}-gallic acid complex usually encased multiple C_{70} molecules due to their mutual *van der Waals* bonding. In water solutions hydrophobic and electrostatic interactions also occurred to reinforce the interactions between C_{70} molecules. These interactions sometimes formed "lacelike" clusters observed in our TEM study. The sizes of these clusters may range from tens of nanometers up to micrometers, similar to that observed for pyridine solubilized C_{60} [16]. With consecutive filtrations to remove free gallic acid and larger C_{70} or C_{70}-gallic acid aggregates, the sizes of C_{70}-gallic acid complexes ranged mostly between 10~20 nm (Figure 1c). Our separate NMR study

found no spectral signatures for C_{70}-gallic acid possibly due to the non-covalent (and therefore random) nature of the binding. The solution of C_{70}-gallic acid exhibited light green color in water and was stable for weeks at room temperature.

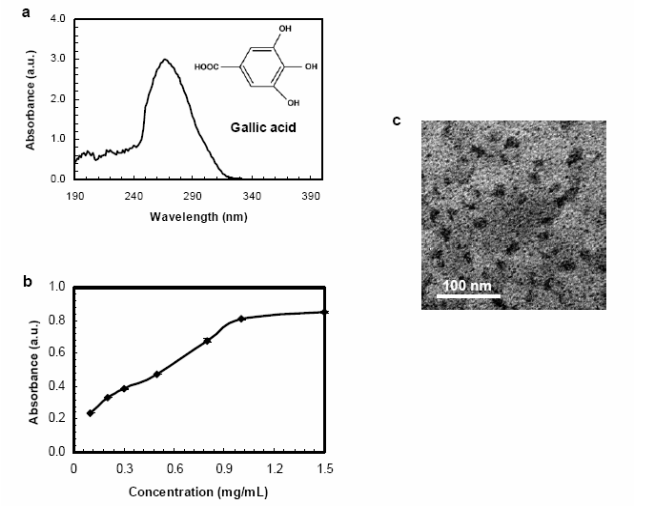

Figure 1: a) Absorption spectrum of gallic acid (structure in inset). b) UV absorbance of C_{70}-gallic acid vs. concentration. c) TEM image of C_{70}-gallic acid complexes.

2.2 Fluorescence of C_{70}-Gallic Acid

The fluorescence spectra of C_{70}-gallic acid were recorded using a spectrofluorometer (Figures 2a and b), and the weight ratio of C_{70} to gallic acid was varied from 1:5 to 1:20, corresponding to a molar ratio of approximate 1/25 to 1/100. As a control, gallic acid of equal amount to the sample yielded only weak fluorescence when excited at 488 nm (grey curve in Figure 2a). In contrast two distinct fluorescence peaks were observed at ~540 nm and 719 nm when the sample (1:5, blue curve) was excited at 488 nm and 690 nm, respectively. This confirms that the fluorescence signals observed at 540 nm and 719 nm were emitted by C_{70} rather than gallic acid. As shown in Figure 2a, centrifugation at 7,500 rpm for 3 min markedly reduced the narrow peak at 719 nm but did not significantly alter the broad fluorescence peak at 540 nm (dark red curve in Figure 2a). This suggests the fluorescence peak at 719 nm was mostly emitted by poorly solubilized C_{70} molecules. This result is similar to that observed for C_{60}-pyridine solutions, where fluorescence peaks at 440 nm, 575 nm, and 700 nm were assigned to C_{60} nanoparticles, C_{60} lace-like clusters, and C_{60} microbulks, respectively [16]. Consistently, the cyan curve (1:20) in Figure 2b exhibits a relatively smaller peak at 719 nm as compared to the orange curve (1:10), possibly due to the higher concentration of gallic acid and therefore improved C_{70} solubility.

Using the same approach we have also solubilized C_{60} with gallic acid in aqueous solutions. However, the fluorescence bands of C_{60}-gallic acid assembly were weaker, much broader, and much less distinctive than their C_{70} counterpart, possibly because the fluorescence emission of C_{60} extends further into the near infrared region [8,9]. These fluorescence characteristics of C_{60}-gallic acid were also more sensitive to particle size and solubilization procedures, which deemed C_{60} less suitable for imaging. Our study in this paper, therefore, focuses on C_{70}-gallic acid only.

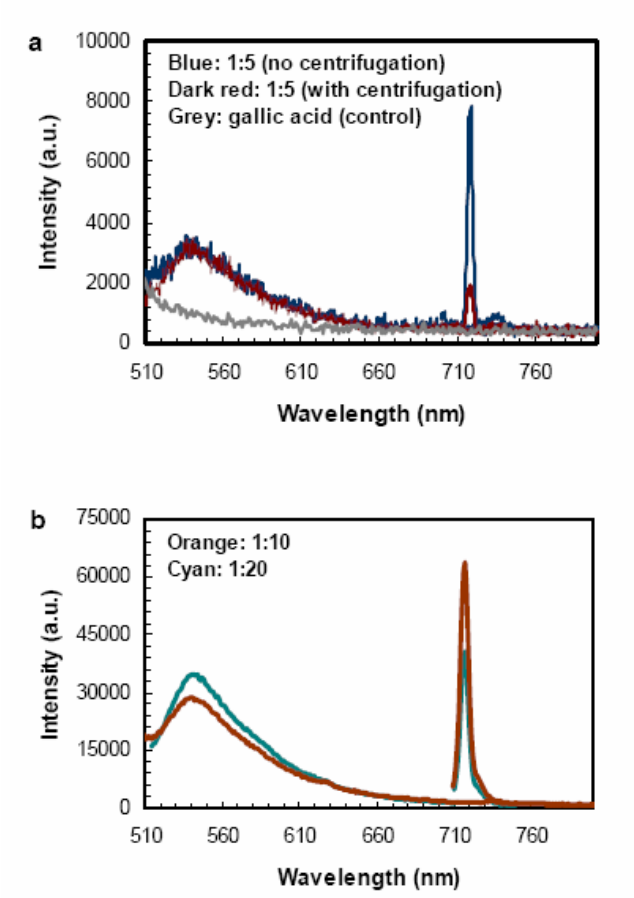

Figure 2: Fluorescence intensity vs. wavelength for C_{70}-gallic acid of different ratios. a) The ratio of C_{70}-gallic acid was set at 1:5 and the concentration of C_{70} was 0.1 mg/mL prior to centrifugation (blue). The fluorescence of gallic acid of equal amount to the sample is shown as control (grey). b) The concentrations of C_{70} were 1 mg/mL for both C_{70}-gallic acid of 1:10 (orange) and 1:20 (cyan). No centrifugation was applied to either case.

2.3 Biological Imaging

One major issue with biological imaging is the photobleaching of fluorophores (e.g. Cy3, TAMRA, and calcein AM), which becomes particularly significant when examining a sample of large dimensions for an extended period of time. For such applications confocal fluorescence microscopy is often employed to utilize its axial sectioning

property, which enables three-dimensional image reconstruction at a later stage. Yet this appealing feature of confocal microscopy is often compromised in practice by the scanning rate, which must be increased to compensate for the rapid photobleaching of sample under irradiation. These fast scanning rates subsequently result in a reduction of both signal strength and image contrast. In the following we show the potential use of C_{70}-gallic acid for long-term and large-scale in vivo imaging.

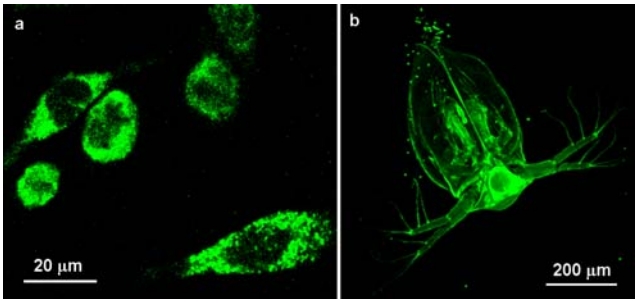

Figure 3: Confocal fluorescence images of C_{70}-gallic acid labeled a) CHO cells and b) living Ceriodaphnia dubia, excited by an Ar+ laser at 488 nm. The CHO cells were incubated with C_{70}-gallic acid for 4 hr and the fluorescence was localized mainly outside the cell nuclei. The Ceriodaphnid was fed with C_{70}-gallic acid for 30 min. The internal organs of the Ceriodaphnid were clearly labeled.

Using a confocal fluorescence microscope (LSM 510, Zeiss) we imaged living Chinese Hamster Ovary (CHO) cells and organism Ceriodaphnia dubia, incubated with C_{70}-gallic acid (Figure 3). Both the interiors and exteriors of the cells were strongly fluorescent excited by an Ar+ laser at 488 nm, suggesting the efficient translocation of C_{70}-gallic acid across cell membranes. However, the green fluorescence was largely excluded by the cell nuclei in Figure 3a possibly due to the relatively large sizes of C_{70}-gallic acid and their dissociation dynamics in the cellular environment. The mechanism of C_{70}-gallic acid uptake will be examined in future studies using fluorescence microscopy and Raman spectroscopy in combination with molecular dynamics simulations. In Figure 3b, the swimming appendages can be seen extended from the cephalothorax surrounding the crustacean's body and the internal organs of the Ceriodaphnid were clearly labeled with C_{70}-gallic acid. The ingestion of C_{70}-gallic acid by Ceriodaphnia and their consequent permeation into tissues is possible. However, since labeling of Ceriodaphnia by C_{70}-gallic acid can be done within minutes, we hypothesize that this internalization route contributed less than the permeation of the nanoparticles through membranes.

Confocal fluorescence imaging has been shown as a powerful tool for the field study of biomineralization [17]. For example the formation of oyster shell depends upon a supply of calcite crystals which are deposited at the mineralization front by the mollusk's immune system cells. Subsequent crystalline growth is mediated by the mantle epithelium resulting in highly organized prismatic and nacreous shell layers [17]. In order to understand the interaction between mineralizing immune systems cells and the mantle it is necessary to perform live imaging of intact oyster tissues. The use of C_{70}-gallic as a bio-imaging reagent enables instantaneous labeling of these tissues for both in vivo and in vitro applications. In comparison with calcein AM, a routine stain for biological imaging, the labeling of C_{70}-gallic acid was less selective (Figure 4a vs. 4c) and far more resistant to irradiation (Figure 4b vs. 4d). The resistance of C_{70}-gallic acid to irradiation allows these nanoparticles to be far more effective than calcein AM for use in examining large tissues and organisms. In addition, calcein AM requires an incubation time of ~20 min for its AM moiety to be cleaved off by intracellular esterases and therefore can only be used for imaging viable samples. In contrast, C_{70}-gallic acid can almost instantaneously label both living and fixed cells or tissues (data not shown) with almost the same efficiency.

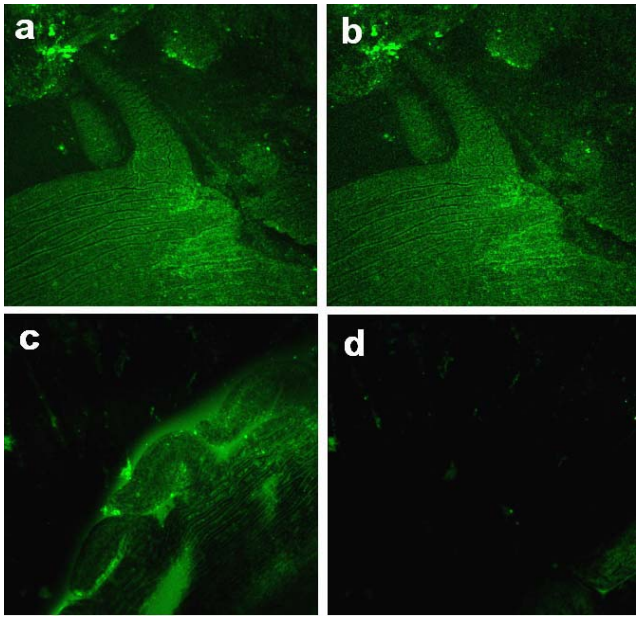

Figure 4: C_{70}-gallic acid labeled living mantle tissue a) before and b) after 4 min of Ar+ laser irradiation. In contrast, c) and d) are calcein AM labeled living mantle tissue c) before and d) after 4 min of laser irradiation.

3 CONCLUSIONS

We have solubilized C_{70} in aqueous solutions using phenol gallic acid, and we hypothesize that the supramolecular complexes of C_{70}-gallic acid are formed via pi-stacking as well as through the caging of gallic acid molecules around C_{70}. The solubility of C_{70} afforded by gallic acid is approximately 1 mg/mL based on our sample preparation procedures. We have also determined that the C_{70}-gallic acid complexes emit multiple fluorescence bands in both

visible and in near infrared. Consequently, we have assigned the 540 nm band to well solubilized C_{70}. Though the mechanism of the robust fluorescence of C_{70}-gallic acid in water is unclear, it is speculated to be related to the degenerated electronic states, reduced symmetry, and the rapid intersystem crossing of C_{70}. Utilizing the fluorescence of C_{70}-gallic acid, we have performed imaging from the cellular to the living organism level. We have shown that the fluorescence of C_{70}-gallic acid is far more resistant to photobleaching and far less selective to the state of biological samples than calcein AM. The uptake mechanism of C_{70}-gallic acid will be examined in our future studies to gain a better understanding of nanomaterial-biological system interaction. However, the free radical generation of pristine fullerenes is of some concern. [18] In principle, this generation can be counterbalanced by gallic acid which is a powerful antioxidant. Since gallic acid is also an anticancer agent and can be further functionalized to incorporate disease specific antibodies, C_{70}-gallic acid has potential uses in a broad array of applications in biosensing, in vivo imaging, therapeutics, and in drug delivery.

4 ACKNOWLEDGEMENTS

Funding of this research was provided by NSF grant No. BES-0630823. We thank JoAn Hudson for assistance with TEM, Brandon Seda for preparing Ceriodaphnia, and Dan Bearden at the Hollings Marine Lab for assistance with NMR.

REFERENCES

[1] L. L. Dugan, D. M. Turetsky, C. Du, Proc. Natl. Acad. Sci. U. S. A. 17, 9434-9439, 1997.
[2] R. Sijbesma, G. Srdanov, F. Wudl, J. A. Castoro, C. Wilkins, S. H. Friedman, D. L. DeCamp, G. L. Kenyon, J. Am. Soc. Chem. 115, 6510-6512, 1993.
[3] N. Gharbi, M. Pressac, M. Hadchouel, H. Szwarc, S. R. Wilson, F. Moussa, Nano Lett. 5, 2578-2585, 2005.
[4] T. Wharton, L. J. Wilson, Tetrahedron Lett. 43, 561-564, 2002.
[5] J. M. Ashcroft, D. A. Tsyboulaski, K. B. Hartman, T. Y. Zakharian, J. W. Marks, R. B. Weisman, M. G. Rosenblum, L. J. Wilson, Chem. Commun. 3004-3006, 2006.
[6] K. C. Hwang, D. Mauzerall, Nature, 361, 138-140, 1993.
[7] S. Niu, D. Mauzerall, J. Am. Soc. Chem. 118, 5791-5795, 1996.
[8] J. W. Arbogast, C. S. Foote, J. Am. Soc. Chem. 113, 8886-8889, 1991.
[9] B. Ma, Y. P. Sun, J. Chem. Soc. Perkin Trans. 2, 2157-2162, 1996.
[10] A. Graja, J. P. Farges, Adv. Mater. Opt. Electron. 8, 215-228, 1998.
[11] K. Harigaya, S. Abe, Phys. Rev. B, 49, 16746-16752, 1994.
[12] K. Harigaya, S. Abe, J. Phys.: Condens. Matter, 8, 8057-8066, 1996.
[13] N. M. Gandhi, C. K. K. Nair, Mol. Cell. Biochem. 278, 111-117, 2005.
[14] M. Labieniec, T. Gabryelak, J. Photochem. Photobiol. B: Biol. 82, 72-78, 2006.
[15] G. V. Andrievsky, V. K. Klochkov, A. Bordyuh, G. I. Dovbeshko, Chem. Phys. Lett. 364, 8-17, 2002.
[16] F. Zhang, Y. Fang, J. Phys. Chem. B, 110, 9022-9026, 2006.
[17] A. S. Mount, A. P. Wheeler, R. P. Paradkar, D. Snider, Science, 304, 297-300, 2004.
[18] C. M. Sayes, J. D. Fortner, W. Guo, D. Lyon, A. M. Boyd, K. D. Ausman, Y. J. Tao, B. Sitharaman, L. J. Wilson, J. B. Hughes, J. L. West, V. L. Colvin, Nano Lett. 4, 1881-1887, 2004.